

Laser Photolysis Studies of the Photochemical Reactions of Chromium(III) Octaethylporphyrin and Tetramesitylporphyrin Complexes in Toluene Solution

Masahiko Inamo,* Kosuke Eba, Kayoko Nakano, and Norio Itoh

Department of Chemistry, Aichi University of Education, Kariya, Aichi 448-8542, Japan

Mikio Hoshino

The Institute of Physical and Chemical Research, Wako, Saitama 351-0189, Japan

Received March 12, 2003

A nanosecond laser photolysis study was carried out for the Cr(III) porphyrin complexes of 2,3,7,8,12,13,17,18-octaethylporphyrin, [Cr(OEP)(Cl)(L)], and of 5,10,15,20-tetramesitylporphyrin, [Cr(TMP)(Cl)(L)], in toluene containing water and an excess amount of L (L = axial ligand). The laser photolysis generates the triplet excited state of the parent complex as well as a five-coordinate complex, [Cr(porphyrin)(Cl)], produced by the photodissociation of the axial ligand L. The yields for the formation of the triplet state and the photodissociation of L are found to markedly depend on the nature of both L and porphyrin ligand. The five-coordinate [Cr(porphyrin)(Cl)] readily reacts with both H₂O and L in the bulk solution to give [Cr(porphyrin)(Cl)(H₂O)] and [Cr(porphyrin)(Cl)(L)], respectively. The axial H₂O ligand in [Cr(porphyrin)(Cl)(H₂O)] is then substituted by the ligand L to regenerate the original complex [Cr(porphyrin)(Cl)(L)]. In principle, the substitution reaction takes place by the dissociative mechanism: the first step is the dissociation of H₂O from [Cr(porphyrin)(Cl)(H₂O)], followed by the reaction of the five-coordinate [Cr(porphyrin)(Cl)] with the ligand L to regenerate [Cr(porphyrin)(Cl)(L)]. The rate constants for this ligand substitution reaction are found to exhibit bell-shaped ligand concentration dependence. The detailed kinetic analysis revealed that both ligands L and H₂O in toluene make a hydrogen bond with the axial H₂O ligand in [Cr(porphyrin)(Cl)(H₂O)] to yield dead-end complexes for the substitution reaction. The reaction mechanisms are discussed on the basis of the substituent effects of the porphyrin peripheral groups and the kinetic parameters determined from the temperature dependence of the rate constants.

Introduction

The roles of natural metalloporphyrins are very important in various biological systems such as electron transfer catalysts of heme-containing enzymes, active sites in heme proteins which reversibly bind dioxygen and carbon monoxide, and the light-harvesting pigments in photosynthetic processes. The photochemistry of synthetic metalloporphyrins has been extensively investigated to elucidate the biological functions of natural metalloporphyrins.¹ Photochemical processes such as photoinduced ligand dissociation are strongly linked with various photophysical processes of the excited-state molecules as luminescence, internal conversion,

intersystem crossing, and intramolecular energy dissipation processes. Thus, studies on the excited states of metalloporphyrins are indispensable for full understanding of photoinduced axial ligand dissociation and association reactions.

We have been particularly interested in the dynamics of the photoinduced axial ligand dissociation and association reaction of the chromium(III) porphyrins. Theoretical and photophysical studies revealed that the excited singlet and triplet states of the porphyrin π system weakly interact with the central chromium atom ($S = 3/2$) to give 4S_1 , 2T_1 , 4T_1 , and 6T_1 excited states and that the lowest and second lowest excited states, 6T_1 and 4T_1 , are in thermal equilibrium.^{2,3} Meanwhile, laser photolysis of chromium(III) porphyrins in

* To whom correspondence should be addressed. E-mail: minamo@aecc.aichi-edu.ac.jp.

(1) Sima, J. *Struct. Bonding* **1995**, *84*, 135.

(2) Gouterman, M.; Hanson, L. K.; Khalil, G.-E.; Leenstra, W. R.; Buchler, J. W. *J. Chem. Phys.* **1975**, *62*, 2343.

(3) Harriman, A. *J. Chem. Soc., Faraday Trans. 1* **1982**, *78*, 2727.

solution causes photoinduced axial ligand ejection as well as other various photoinduced phenomena.^{4–11} Since the photodissociated ligand undergoes a recombination reaction to yield the parent metalloporphyrins, laser photolysis is one of the key methods to elucidate the dynamics of the axial ligand binding. An earlier study has shown that the axial ligand of chromium(III) porphyrins is fairly labile compared with those of other chromium(III) complexes having non-porphyrin ligands.⁶ The high reactivity of the chromium(III) porphyrins coupled with the facile ligand substitution reaction at the axial coordination site is of fundamental interest for their chemistry in solution.^{12–24}

The electronic structure and the reactivity of the metalloporphyrins in the excited and ground states are strongly affected by the nature of the axial ligand as well as the molecular structure of the porphyrin ligand.²⁵ However, little information is available on the relationship between the porphyrin structure and the photochemical and photophysical properties of the chromium(III) porphyrins. As a continuing effort to develop our understanding of chromium(III) porphyrin chemistry, we have investigated the photochemistry of complexes of 2,3,7,8,12,13,17,18-octaethylporphyrin, [Cr(OEP)(Cl)(L)], and of 5,10,15,20-tetramesitylporphyrin, [Cr(TMP)(Cl)(L)], in toluene (L = axial ligand) using a nanosecond laser photolysis technique. In this paper, we describe the mechanism of the photoinduced reactions of these chromium(III) porphyrins on the basis of the kinetics of the reaction and the quantum yield measurements to gain further insight into the properties of the excited states responsible for the photoinduced dissociation of the axial ligand.

Experimental Section

Chloro(2,3,7,8,12,13,17,18-octaethylporphyrinato)chromium(III), [Cr(OEP)(Cl)(H₂O)] (**1**), and chloro(5,10,15,20-tetramesitylporphyrinato)chromium(III), [Cr(TMP)(Cl)(H₂O)] (**2**), were prepared and purified according to the synthetic procedure for the chromium(III) 5,10,15,20-tetraphenylporphyrin complex [Cr(TPP)(Cl)(H₂O)].^{6,26} Pyridine (Py, Wako Pure Chemicals) and 1-methylimidazole (1-MeIm, Wako Pure Chemicals) were dried over solid potassium hydroxide and then distilled. 3-Cyanopyridine (3-CNPy, Wako Pure Chemicals) was purified by vacuum sublimation. Toluene (Wako Pure Chemicals) was dried over sodium metal and then distilled. Anal. Calcd (found) for **1** (C₃₆H₄₆ClCrN₄O): C, 67.17 (67.75); H, 7.26 (7.32); N, 8.78 (8.43); Cl, 5.55 (5.67). Calcd (found) for **2** (C₅₆H₅₄ClCrN₄O·0.27CHCl₃): C, 73.56 (73.53); H, 5.95 (6.29); N, 6.10 (6.02).

Absorption spectra were recorded on a Hitachi U-3000 spectrophotometer. A cryostat (Oxford DN1704) was used to measure the absorption spectra at low temperatures. Laser photolysis studies were carried out with a Nd:YAG laser (Surelite, Hoya-Continuum) equipped with the second (532 nm) harmonic generator. The duration of the 532 nm pulse was 6 ns. The detection system of the transient spectra was described previously.⁶ The concentration of the chromium(III) porphyrin complex in toluene was less than 1.0×10^{-5} mol kg⁻¹, and that of the axial ligand, more than 1.0×10^{-4} mol kg⁻¹. The concentration of water in the toluene solution was determined by a Karl Fischer titrator (CA-06, Mitsubishi Chemicals). The O₂ concentration in toluene solutions was determined by measuring the O₂ pressure with a mercury manometer. The Bunsen coefficient of O₂ in toluene is 0.22 at 25.0 °C.²⁷ Polystyrene films dissolved chromium(III) porphyrins were prepared according to the method previously reported.⁷

The experimental pseudo-first-order rate constant k_{obsd} was obtained from the nonlinear least-squares analysis of the transient-decay curve observed after the laser pulse. The decay curves were averaged several times on the digital oscilloscope. The estimated standard deviation of k_{obsd} was less than $\pm 3\%$.

The experimental pseudo-first-order rate constant k_{obsd} was obtained from the nonlinear least-squares analysis of the transient-decay curve observed after the laser pulse. The decay curves were averaged several times on the digital oscilloscope. The estimated standard deviation of k_{obsd} was less than $\pm 3\%$.

Results

Photoreaction of [Cr(OEP)(Cl)(H₂O)] and [Cr(TMP)(Cl)(H₂O)]. We previously reported that the chromium(III) tetraphenylporphyrin complex exists as [Cr(TPP)(Cl)(H₂O)] (TPP = 5,10,15,20-tetraphenylporphyrin) in a toluene solution containing 1×10^{-3} mol kg⁻¹ water.⁶ Laser irradiation causes the photodissociation of H₂O from [Cr(TPP)(Cl)(H₂O)], followed by the recombination reaction with H₂O to regenerate the initial complex. In the present study, similar experiments were performed for the OEP and TMP complexes. UV–visible absorption spectra are shown in Figure 1 for [Cr(TMP)(Cl)(H₂O)] and in Figure S1 for [Cr(OEP)(Cl)(H₂O)], together with the transient spectra observed after the laser pulse. The spectrum of [Cr(TMP)(Cl)(H₂O)] reversibly changes with temperature, and a new Soret band appears in the 430 nm region with an increase in the temperature. In the inset of Figure 1, the transient spectrum observed after the laser pulse is shown together with the difference spectrum obtained by subtracting the spectrum measured at -40 °C from that at 40 °C. These two spectra are almost identical, and therefore the blue-shifted band observed at the higher temperatures can be attributed to the five-coordinate species,

- (4) Yamaji, M.; Hama, Y.; Hoshino, M. *Chem. Phys. Lett.* **1990**, *165*, 309.
- (5) Yamaji, M. *Inorg. Chem.* **1991**, *30*, 2949.
- (6) Inamo, M.; Hoshino, M.; Nakajima, K.; Aizawa, S.; Funahashi, S. *Bull. Chem. Soc. Jpn.* **1995**, *68*, 2293.
- (7) Hoshino, M.; Tezuka, N.; Inamo, M. *J. Phys. Chem.* **1996**, *100*, 627.
- (8) Hoshino, M.; Nagamori, T.; Seki, H.; Chihara, T.; Tase, T.; Wakatsuki, Y.; Inamo, M. *J. Phys. Chem. A* **1998**, *102*, 1297.
- (9) Inamo, M.; Hoshino, M. *Photochem. Photobiol.* **1999**, *70*, 596.
- (10) Inamo, M.; Nakaba, H.; Nakajima, K.; Hoshino, M. *Inorg. Chem.* **2000**, *39*, 4417.
- (11) Jeoung, S. C.; Kim, D.; Cho, D. W.; Yoon, M. *J. Phys. Chem. A* **2000**, *104*, 4816.
- (12) Fleischer, E. B.; Krishnamurthy, M. *J. Am. Chem. Soc.* **1971**, *93*, 3784.
- (13) Fleischer, E. B.; Krishnamurthy, M. *J. Coord. Chem.* **1972**, *2*, 89.
- (14) Krishnamurthy, M. *Inorg. Chim. Acta* **1978**, *26*, 137.
- (15) Ashley, K. R.; Leipoldt, J. G.; Joshi, V. K. *Inorg. Chem.* **1980**, *19*, 1608.
- (16) Leipoldt, J. G.; Basson, S. S.; Rabie, D. R. *J. Inorg. Nucl. Chem.* **1981**, *43*, 3239.
- (17) O'Brien P.; Sweigart, D. A. *Inorg. Chem.* **1982**, *21*, 2094.
- (18) Leipoldt, J. G.; van Eldik, R.; Kelm, H. *Inorg. Chem.* **1983**, *22*, 4146.
- (19) Leipoldt, J. G.; Meyer, H. *Polyhedron* **1987**, *6*, 1361.
- (20) Ashley, K. R.; Kuo, J. *Inorg. Chem.* **1988**, *27*, 3556.
- (21) Ashley, K. R.; Trent, I. *Inorg. Chim. Acta* **1989**, *163*, 159.
- (22) Inamo, M.; Sumi, T.; Nakagawa, N.; Funahashi, S.; Tanaka, M. *Inorg. Chem.* **1989**, *28*, 2688.
- (23) Inamo, M.; Sugiura, S.; Fukuyama, H.; Funahashi, S. *Bull. Chem. Soc. Jpn.* **1994**, *67*, 1848.
- (24) Inamo, M.; Nakajima, K. *Bull. Chem. Soc. Jpn.* **1998**, *71*, 883.
- (25) Gouterman, M. In *The Porphyrins*; Dolphin, D., Ed.; Academic Press: New York, 1978; Vol. III, Chapter 1.

(26) Summerville, D. A.; Jones, R. D.; Hoffman, B. M.; Basolo, F. *J. Am. Chem. Soc.* **1977**, *99*, 8195.

(27) Battino, R., Ed. *IUPAC Solubility Data Series*; Pergamon Press: Oxford, U.K., 1981; Vol. 7.

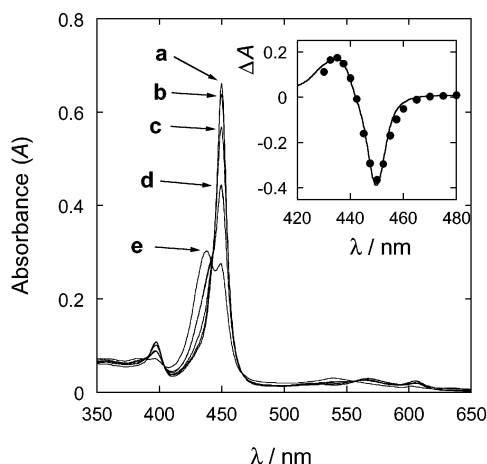
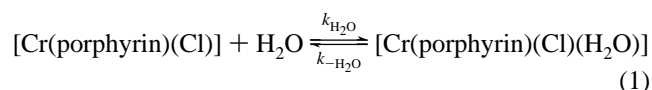


Figure 1. UV-visible absorption spectra of the toluene solution of the Cr(III)-TMP complex. $T/^\circ\text{C} = -40$ (a), -20 (b), 0 (c), 20 (d), and 40 (e). $[\text{H}_2\text{O}] = 4.24 \times 10^{-3} \text{ mol kg}^{-1}$. In the inset, the transient spectrum of the toluene solution of the Cr(III)-TMP complex observed just after the laser irradiation (●) and the differences between the spectrum of the Cr(III)-TMP complex measured at 40°C and that measured at -40°C (solid line) are shown.

$[\text{Cr}(\text{TMP})(\text{Cl})]$. On the other hand, the spectral changes are not found for $[\text{Cr}(\text{OEP})(\text{Cl})(\text{H}_2\text{O})]$ in the temperature range from -40 to 40°C . These findings indicate that the H_2O molecule in $[\text{Cr}(\text{OEP})(\text{Cl})(\text{H}_2\text{O})]$ binds to the central Cr(III) atom more tightly than that in $[\text{Cr}(\text{TMP})(\text{Cl})(\text{H}_2\text{O})]$.

The transient spectra shown in Figure 1 and Figure S1 decay according to first-order kinetics without the formation of permanent photoproducts. Figure 2 shows the plots of the pseudo-first-order rate constants, k_{obsd} , for the decay of the transient spectra represented as a function of the water concentration. The pseudo-first-order rate constant increases with an increase in the water concentration. These observations indicate that the five-coordinate species, $[\text{Cr}(\text{TMP})(\text{Cl})]$ and $[\text{Cr}(\text{OEP})(\text{Cl})]$, produced by the laser photolysis undergo the recombination reaction with H_2O , returning to the six-coordinate species, $[\text{Cr}(\text{TMP})(\text{Cl})(\text{H}_2\text{O})]$ and $[\text{Cr}(\text{OEP})(\text{Cl})(\text{H}_2\text{O})]$. The decay of the transient spectrum can be attributed to the following:



Thus, k_{obsd} is given by

$$k_{\text{obsd}} = k_{\text{H}_2\text{O}}[\text{H}_2\text{O}] + k_{-\text{H}_2\text{O}} \quad (2)$$

where $k_{\text{H}_2\text{O}}$ and $k_{-\text{H}_2\text{O}}$ represent the second-order rate constant for the water association reaction and the first-order rate constant for the water dissociation reaction, respectively. The plots of k_{obsd} vs $[\text{H}_2\text{O}]$ in Figure 2 give straight lines in appearance. However, as will be mentioned later, the reaction 1 is more or less complicated due to the existence of $[\text{Cr}(\text{porphyrin})(\text{Cl})(\text{HOH}\cdots\text{OH}_2)]$, in which a water molecule is bound to the coordinate H_2O ligand by hydrogen bonding. The detailed kinetic analysis will be described later.

The intercept of the line in Figure 2 for the TMP complex is larger than that of the OEP complex, indicating that the

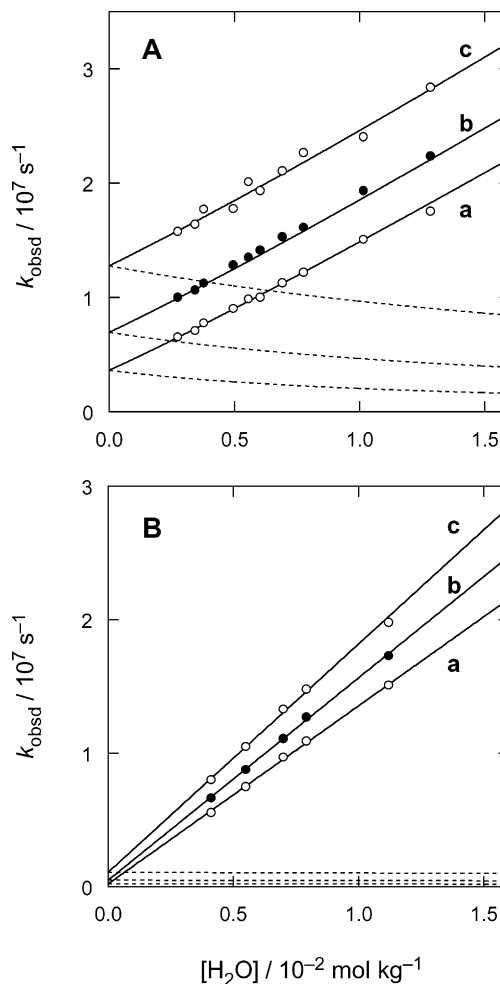


Figure 2. Dependence of the pseudo-first-order rate constant k_{obsd} of the decay of the transient spectrum for $[\text{Cr}(\text{porphyrin})(\text{Cl})(\text{H}_2\text{O})]$ on the concentration of H_2O in toluene for the TMP (A) and OEP (B) complexes. $T/^\circ\text{C} = 15.0$ (a), 25.0 (b), and 35.0 (c). Solid and dotted lines represent the calculated curves for eq 12 and the second term of the right-hand side of eq 12, respectively.

axial H_2O in $[\text{Cr}(\text{TMP})(\text{Cl})(\text{H}_2\text{O})]$ dissociates more easily than that in $[\text{Cr}(\text{OEP})(\text{Cl})(\text{H}_2\text{O})]$. This is supported by the facts that, as shown in Figure 1, the TMP complex in toluene exists as the mixture of $[\text{Cr}(\text{TMP})(\text{Cl})(\text{H}_2\text{O})]$ and $[\text{Cr}(\text{TMP})(\text{Cl})]$ when $[\text{H}_2\text{O}] = 4.24 \times 10^{-3} \text{ mol kg}^{-1}$ and that the OEP complex exists solely as $[\text{Cr}(\text{OEP})(\text{Cl})(\text{H}_2\text{O})]$.

We observed merely the photodissociation of the axial H_2O from $[\text{Cr}(\text{porphyrin})(\text{Cl})(\text{H}_2\text{O})]$. No any other transient species such as the excited state of the five-coordinate complex, $[\text{Cr}(\text{porphyrin})(\text{Cl})]$, or the triplet excited state of $[\text{Cr}(\text{porphyrin})(\text{Cl})(\text{H}_2\text{O})]$ could be detected. These findings indicate that the lifetimes of these excited states are too short to be observed by the present nanosecond laser photolysis technique.

Photoreaction of $[\text{Cr}(\text{OEP})(\text{Cl})(\text{L})]$ ($\text{L} = \text{Py}$, 1-MeIm). The chromium(III) porphyrins exist as $[\text{Cr}(\text{porphyrin})(\text{Cl})(\text{L})]$ in the toluene solution containing an excess amount of a ligand L such as Py and 1-MeIm. Figure 3 shows the transient spectra for $[\text{Cr}(\text{OEP})(\text{Cl})(\text{Py})]$ and $[\text{Cr}(\text{OEP})(\text{Cl})(1\text{-MeIm})]$ in toluene and in polystyrene film observed after a 532-nm laser irradiation. In the polystyrene film, the transient species of the 1-MeIm complex has a strong

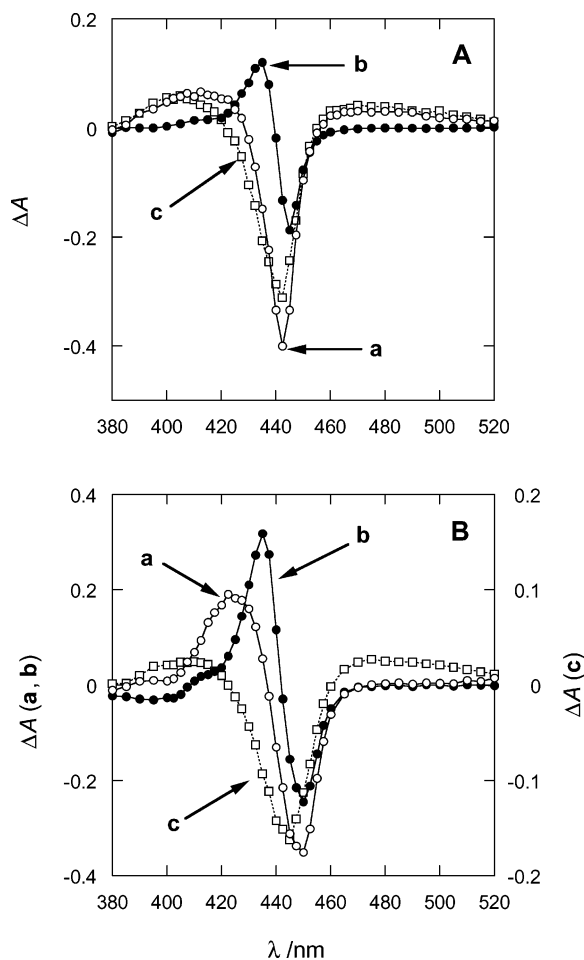


Figure 3. Transient spectra observed for the toluene solution of $[\text{Cr}(\text{OEP})(\text{Cl})(1\text{-MeIm})]$ in the presence of $5.82 \times 10^{-3} \text{ mol kg}^{-1}$ 1-MeIm and $5.87 \times 10^{-3} \text{ mol kg}^{-1}$ H_2O (A) and for that of $[\text{Cr}(\text{OEP})(\text{Cl})(\text{Py})]$ in the presence of $4.03 \times 10^{-3} \text{ mol kg}^{-1}$ Py and $5.29 \times 10^{-3} \text{ mol kg}^{-1}$ H_2O (B) at 25.0°C . The spectra were taken at 29 ns (a) and 690 ns (b) for (A) and at 29 ns (a) and 725 ns (b) for (B) after a 532 nm laser irradiation. The transient spectra observed for the polystyrene film containing $[\text{Cr}(\text{OEP})(\text{Cl})(1\text{-MeIm})]$ taken at 59 ns and that of $[\text{Cr}(\text{OEP})(\text{Cl})(\text{Py})]$ taken at 229 ns are also shown as spectrum c for each case.

negative absorption around 440 nm. Since the photodissociation of the axial ligand of the complex does not occur in the polystyrene film, this species can be ascribed to the ${}^6\text{T}_1$ excited state of $[\text{Cr}(\text{OEP})(\text{Cl})(1\text{-MeIm})]$, which is in thermal equilibrium with the ${}^4\text{T}_1$ state.^{2,7} The triplet excited state, ${}^6\text{T}_1$, decays according to first-order kinetics with a rate constant of $3.7 \times 10^6 \text{ s}^{-1}$ at 25.0°C . On the other hand, the decay of the transient spectrum in the toluene solution was found to be biphasic. The faster step of the decay, which we call the “fast process”, is completed within 10^{-6} s after the laser pulse, and a much slower process (“slow process”) follows it. As shown in Figure 3A, the transient spectrum in the toluene solution measured at 29 ns after the laser pulse is similar to that in the polystyrene film with a slight difference around the 430 nm region. These findings indicate that, as in the case of $[\text{Cr}(\text{TPP})(\text{Cl})(\text{Py})]$,⁹ the transient spectrum measured at 29 ns can be ascribed to both the triplet excited state of $[\text{Cr}(\text{OEP})(\text{Cl})(1\text{-MeIm})]$ and the five-coordinate species $[\text{Cr}(\text{OEP})(\text{Cl})]$ given by the photodissociation of 1-MeIm from $[\text{Cr}(\text{OEP})(\text{Cl})(1\text{-MeIm})]$ in toluene.

The latter species corresponds to the difference between the transient spectrum in the polystyrene film (spectrum c in Figure 3A) and that in the toluene solution (spectrum a in Figure 3A). The second transient spectrum of $[\text{Cr}(\text{OEP})(\text{Cl})(1\text{-MeIm})]$ in the toluene solution measured at 690 ns after the laser pulse (spectrum b in Figure 3A) is in good agreement with the difference spectrum between $[\text{Cr}(\text{OEP})(\text{Cl})(\text{H}_2\text{O})]$ and $[\text{Cr}(\text{OEP})(\text{Cl})(1\text{-MeIm})]$ in toluene as shown in Figure S2. Thus, the second transient species is ascribed to $[\text{Cr}(\text{OEP})(\text{Cl})(\text{H}_2\text{O})]$, which is produced by the reaction between the transient $[\text{Cr}(\text{OEP})(\text{Cl})]$ and H_2O . The intermediate, $[\text{Cr}(\text{OEP})(\text{Cl})(\text{H}_2\text{O})]$, eventually returns to $[\text{Cr}(\text{OEP})(\text{Cl})(1\text{-MeIm})]$ by the axial ligand substitution reaction with 1-MeIm in the solution. The photophysical and photochemical processes of $[\text{Cr}(\text{OEP})(\text{Cl})(1\text{-MeIm})]$ are similar to that of $[\text{Cr}(\text{TPP})(\text{Cl})(\text{Py})]$,¹⁰ and the reaction mechanism can be expressed by Scheme 1.

According to Scheme 1, the fast process includes four processes, i.e., the dissociation of the axial ligand from the triplet excited state (k_{diss}), intersystem crossing of the triplet excited state to the ground singlet state ($k_{\text{T-S}}$), and the reactions of the five-coordinate complex $[\text{Cr}(\text{OEP})(\text{Cl})]$ with H_2O ($k_{\text{H}_2\text{O}}$) and 1-MeIm (k_{L}).

The transient spectrum observed for $[\text{Cr}(\text{OEP})(\text{Cl})(\text{Py})]$ decays via a biphasic process as shown in Figure 3. The typical absorption band of the triplet excited state around 480 nm was not observed in the transient spectrum taken at 29 ns after the laser pulse (spectrum a in Figure 3B), while the absorption band around 430 nm, which can be attributed to the five-coordinate $[\text{Cr}(\text{OEP})(\text{Cl})]$, is much more intense than that observed for $[\text{Cr}(\text{OEP})(\text{Cl})(1\text{-MeIm})]$. These findings indicate that the quantum yield for the photodissociation of the axial Py ligand in the singlet excited state is so high that the intersystem crossing leading to the generation of the triplet excited state becomes negligible or that the lifetime of the triplet excited state is extremely short due to the efficient photodissociation of the axial Py ligand. From these results, we conclude that the first transient detected at 29 ns after the pulse is solely ascribed to the five-coordinate $[\text{Cr}(\text{OEP})(\text{Cl})]$. Since the second transient spectrum taken at 725 ns after the pulse is quite similar to the difference spectrum between $[\text{Cr}(\text{OEP})(\text{Cl})(\text{H}_2\text{O})]$ and $[\text{Cr}(\text{OEP})(\text{Cl})(\text{Py})]$, the second transient is attributed to $[\text{Cr}(\text{OEP})(\text{Cl})(\text{H}_2\text{O})]$. The decay of the first transient spectrum to the second one obeys first-order kinetics with respect to the complex, and it corresponds to the reaction of $[\text{Cr}(\text{OEP})(\text{Cl})]$ with Py and H_2O in the bulk solution to generate $[\text{Cr}(\text{OEP})(\text{Cl})(\text{Py})]$ and $[\text{Cr}(\text{OEP})(\text{Cl})(\text{H}_2\text{O})]$, respectively. Reaction paths (k_{diss} and $k_{\text{T-S}}$) for the triplet excited state are missing from the fast process of the Py complex due to the quite low quantum yield of the triplet excited state.

Photoreaction of $[\text{Cr}(\text{TMP})(\text{Cl})(\text{L})]$ ($\text{L} = \text{Py}, 1\text{-MeIm}$). The transient spectra observed for $[\text{Cr}(\text{TMP})(\text{Cl})(\text{Py})]$ in toluene and in a polystyrene film after a 532-nm laser pulse are shown in Figure 4. In the polystyrene film, the transient species ascribed to the triplet excited states (${}^6\text{T}_1$ and ${}^4\text{T}_1$) of $[\text{Cr}(\text{TMP})(\text{Cl})(\text{Py})]$ decays according to first-order kinetics with a rate constant of $8.0 \times 10^6 \text{ s}^{-1}$ at 25.0°C without the

Scheme 1

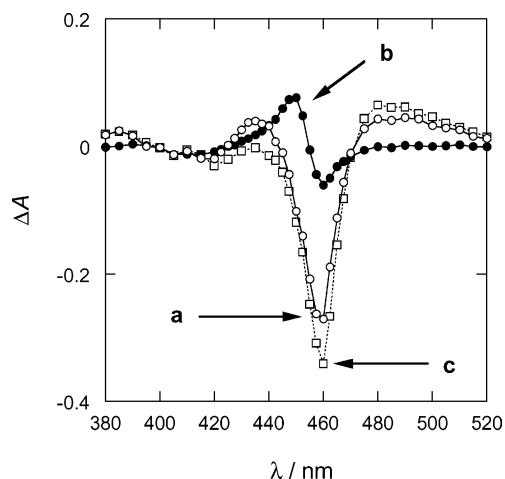
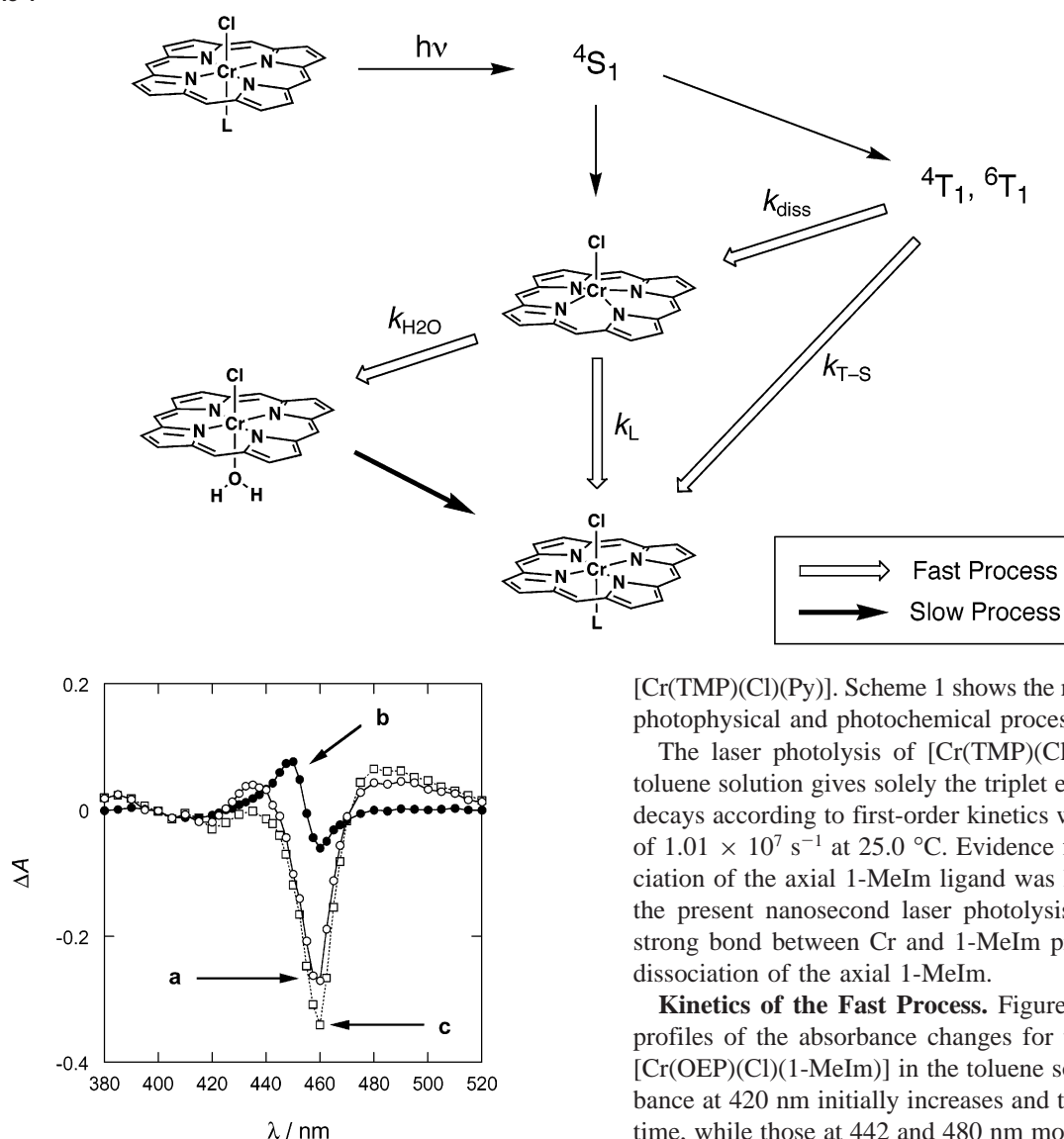


Figure 4. Transient spectra observed for the toluene solution of $[\text{Cr}(\text{TMP})(\text{Cl})(\text{Py})]$ in the presence of $7.55 \times 10^{-3} \text{ mol kg}^{-1}$ Py and $5.38 \times 10^{-3} \text{ mol kg}^{-1}$ H_2O at 25.0°C . The spectra were taken at 29 ns (a) and 483 ns (b) after a 532 nm laser irradiation. The transient spectrum observed for the polystyrene film containing $[\text{Cr}(\text{TMP})(\text{Cl})(\text{Py})]$ taken at 39 ns is also shown (c).

dissociation of the axial ligand. On the other hand, as in the case of the OEP complex, the decay of the transient spectrum in the toluene solution containing excess water and pyridine was found to be biphasic. The fast step of the decay is completed within 10^{-6} s after the laser pulse, followed by a much slower reaction. The first transient spectrum measured at 29 ns after the laser pulse indicates that both the triplet excited state of $[\text{Cr}(\text{TMP})(\text{Cl})(\text{Py})]$ and the five-coordinate species $[\text{Cr}(\text{TMP})(\text{Cl})]$ are produced by the laser photolysis of $[\text{Cr}(\text{TMP})(\text{Cl})(\text{Py})]$. The second transient spectrum in the toluene solution measured at 483 ns after the laser pulse is in good agreement with the difference spectrum between $[\text{Cr}(\text{TMP})(\text{Cl})(\text{H}_2\text{O})]$ and $[\text{Cr}(\text{TMP})(\text{Cl})(\text{Py})]$. Thus, the second transient species is ascribed to $[\text{Cr}(\text{TMP})(\text{Cl})(\text{H}_2\text{O})]$. The axial ligand substitution reaction of $[\text{Cr}(\text{TMP})(\text{Cl})(\text{H}_2\text{O})]$ with pyridine regenerates the parent complex,

$[\text{Cr}(\text{TMP})(\text{Cl})(\text{Py})]$. Scheme 1 shows the mechanism of these photophysical and photochemical processes.

The laser photolysis of $[\text{Cr}(\text{TMP})(\text{Cl})(1\text{-MeIm})]$ in the toluene solution gives solely the triplet excited state, which decays according to first-order kinetics with a rate constant of $1.01 \times 10^7 \text{ s}^{-1}$ at 25.0°C . Evidence for the photodissociation of the axial 1-MeIm ligand was hardly obtained by the present nanosecond laser photolysis. Presumably, the strong bond between Cr and 1-MeIm prohibits the photodissociation of the axial 1-MeIm.

Kinetics of the Fast Process. Figure 5 shows the time profiles of the absorbance changes for the fast process of $[\text{Cr}(\text{OEP})(\text{Cl})(1\text{-MeIm})]$ in the toluene solution. The absorbance at 420 nm initially increases and then decreases with time, while those at 442 and 480 nm monotonically change with time, indicating that consecutive reactions are included in the fast process. On the basis of the mechanism shown in Scheme 1, the first and second of these consecutive reactions are attributed to the decay of the triplet excited state and the reaction of the five-coordinate intermediate $[\text{Cr}(\text{OEP})(\text{Cl})]$ with 1-MeIm or H_2O , respectively. The spectral changes in the range between 380 and 520 nm were analyzed using the SPECFIT/32 program with a kinetic model of consecutive reactions, $\text{A} \rightarrow \text{B} \rightarrow \text{C}$, and the rate constants of each process were determined.^{28,29} The values of the pseudo-first-order rate constants of each reaction, i.e., k_{obsd1} for the reaction $\text{A} \rightarrow \text{B}$ and k_{obsd2} for the reaction $\text{B} \rightarrow \text{C}$, were determined as $k_{\text{obsd1}} = 3.9 \times 10^7 \text{ s}^{-1}$ and $k_{\text{obsd2}} = 9.2 \times 10^6 \text{ s}^{-1}$ ($T = 25.0^\circ\text{C}$). k_{obsd1} can be expressed as $k_{\text{obsd1}} = k_{\text{T-S}} + k_{\text{diss}}$ on the basis of the mechanism of Scheme 1. The rate constant, $3.7 \times 10^6 \text{ s}^{-1}$, for the decay of the triplet excited state of $[\text{Cr}(\text{OEP})(\text{Cl})(1\text{-MeIm})]$ in the polystyrene film is smaller than k_{obsd1} in toluene because the reaction in the solid matrix

(28) Gampp, H.; Maeder, M.; Meyer, C. J.; Zuberbühler, A. D. *Talanta* **1985**, *32*, 95.

(29) SPECFIT/32; Spectrum Software Associates: Marlborough, MA.

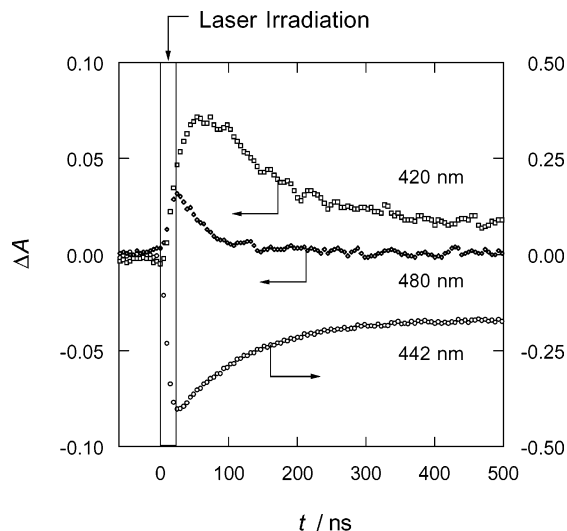


Figure 5. Change in absorbance of the toluene solution of [Cr(OEP)(Cl)(1-MeIm)] caused by a 532 nm laser irradiation. Conditions are the same as those of Figure 3.

does not include the dissociation of the axial 1-MeIm ligand. Meanwhile, $k_{\text{obsd}2}$ is given by $k_{\text{H}_2\text{O}}[\text{H}_2\text{O}] + k_{1\text{-MeIm}}[1\text{-MeIm}]$. Second-order rate constants, $k_{\text{H}_2\text{O}}$ and $k_{1\text{-MeIm}}$, can be determined from the kinetic analysis of the slow process for the photoreaction of [Cr(OEP)(Cl)(1-MeIm)]. As will be mentioned in the next section, we obtained $k_{\text{H}_2\text{O}} = 1.52 \times 10^9 \text{ mol}^{-1} \text{ kg s}^{-1}$ and $k_{1\text{-MeIm}} = 5.56 \times 10^8 \text{ mol}^{-1} \text{ kg s}^{-1}$ at $T = 25.0 \text{ }^\circ\text{C}$. The $k_{\text{obsd}2}$ value, $1.2 \times 10^7 \text{ s}^{-1}$, calculated by using these values, $[\text{H}_2\text{O}] = 5.87 \times 10^{-3} \text{ mol kg}^{-1}$ and $[1\text{-MeIm}] = 5.82 \times 10^{-3} \text{ mol kg}^{-1}$, agrees well with the value determined by the present SPECFIT/32 analysis.

This analysis also provides the spectra of each species as the difference spectrum (transient species minus [Cr(OEP)(Cl)(1-MeIm)]). The transient spectra obtained are shown in Figure S5. It is found that the triplet excited state of [Cr(OEP)(Cl)(1-MeIm)] in toluene (spectrum a in Figure S5) has almost the same spectrum as that in the polystyrene film (spectrum d in Figure S5). The spectrum of [Cr(OEP)(Cl)] (spectrum b in Figure S5) has a positive peak around 420 nm and bleaching of the Soret band of the parent complex, indicating that the Soret band is blue shifted due to the dissociation of the axial ligand.

For the fast process of the photoreaction of [Cr(TMP)(Cl)(Py)] in toluene, SPECFIT/32 analysis could not be successful probably because of the complicated decay profile owing to the overlaps of the fast process and the following ligand substitution reaction, which will be mentioned later.

Kinetics of the Slow Process. As mentioned above, the slow process can be ascribed to the axial water substitution reaction of the intermediate, [Cr(porphyrin)(Cl)(H₂O)], by the nitrogenous base L in the solution. The pseudo-first-order rate constant, k_{obsd} , of the axial substitution reaction was measured in the presence of an excess amount of L. Figure 6 shows the plots of the rate constant k_{obsd} vs [Py] at several concentrations of H₂O, obtained for the slow process of the photoreaction of [Cr(TMP)(Cl)(Py)] in toluene at 25.0 °C. Results obtained at 15.0 and 35.0 °C are shown in Figure S6. We previously reported the kinetics of the axial water

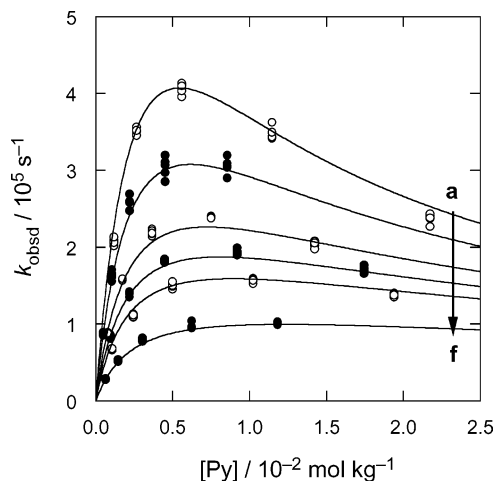
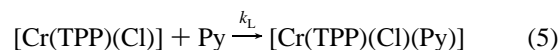
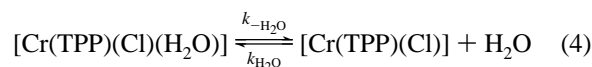
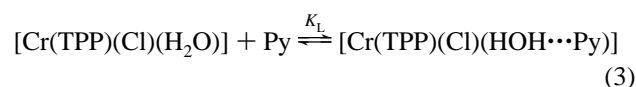


Figure 6. Plot of the pseudo-first-order rate constant k_{obsd} of the decay of [Cr(TMP)(Cl)(H₂O)] as a function of the concentration of pyridine for the laser photolysis of [Cr(TMP)(Cl)(Py)] in toluene. $C_{\text{H}_2\text{O}}/\text{mol kg}^{-1} = 3.1 \times 10^{-3}$ (a), 4.7×10^{-3} (b), 7.1×10^{-3} (c), 9.1×10^{-3} (d), 1.11×10^{-2} (e), and 1.91×10^{-2} (f). $T = 25.0 \text{ }^\circ\text{C}$.

substitution reaction of [Cr(TPP)(Cl)(H₂O)] by a ligand L such as pyridine.¹⁰ This reaction was found to occur according to the dissociative mechanism with a dead-end complex formation as a preequilibrium of the substitution reaction:

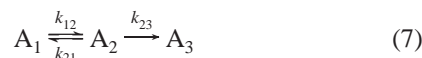


The dead-end complex, [Cr(TPP)(Cl)(HOH⋯Py)], represents the complex in which the Py molecule binds to the hydrogen atom of the coordinating H₂O ligand in [Cr(TPP)(Cl)(H₂O)] by hydrogen bonding. By application of the steady-state approximation to the five-coordinate intermediate, [Cr(TPP)(Cl)], the pseudo-first-order rate constant, k_{obsd} , is formulated as

$$k_{\text{obsd}} = k_{-\text{H}_2\text{O}}k_{\text{L}}[\text{Py}](k_{\text{H}_2\text{O}}[\text{H}_2\text{O}] + k_{\text{L}}[\text{Py}])^{-1}(1 + K_{\text{L}}[\text{Py}])^{-1} \quad (6)$$

The axial water substitution reactions of the TMP and OEP complexes by L are expected to occur via a similar dissociative mechanism. However, the kinetic results shown in Figure 6 and Figure S6 could not be satisfactorily explained by eq 6,³⁰ indicating that the steady-state approximation to the five-coordinate intermediate is inappropriate in the present case. This is because the assumptions used in the steady-state approximation, i.e., $k_{-\text{H}_2\text{O}} \ll k_{\text{H}_2\text{O}}[\text{H}_2\text{O}]$ and $k_{-\text{H}_2\text{O}} \ll k_{\text{L}}[\text{L}]$, are not satisfied due to relatively large $k_{-\text{H}_2\text{O}}$ value for the TMP complex. Instead, the consecutive reactions were considered:

(30) Maximum deviation between the obtained rate constant and the calculated value based on eq 6 exceeds 30%.



Here A_1 , A_2 , and A_3 correspond to $[\text{Cr}(\text{TMP})(\text{Cl})(\text{H}_2\text{O})]$, $[\text{Cr}(\text{TMP})(\text{Cl})]$, and $[\text{Cr}(\text{TMP})(\text{Cl})(\text{L})]$, respectively.^{31,32} In eq 7, the backward reaction from A_3 to A_2 was neglected because the rate constant is extremely smaller than k_{12} , k_{21} , and k_{23} .³³ When the concentration of Py is high and thus the chromium species is completely transformed to $[\text{Cr}(\text{TMP})(\text{Cl})(\text{L})]$, the absorbance of the reacting solution, A , can be expressed as

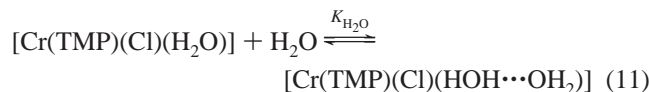
$$A = P \exp(-\lambda_2 t) + Q \exp(-\lambda_3 t) + R \quad (8)$$

$$\lambda_2 = 0.5\{k_{12} + k_{21} + k_{23} + [(k_{12} + k_{21} + k_{23})^2 - 4k_{12}k_{23}]^{1/2}\} \quad (9)$$

$$\lambda_3 = 0.5\{k_{12} + k_{21} + k_{23} - [(k_{12} + k_{21} + k_{23})^2 - 4k_{12}k_{23}]^{1/2}\} \quad (10)$$

where terms P , Q , and R are the functions of the rate constants (k_{12} , k_{21} , k_{23}), molar absorption coefficients of each species, and the initial concentration of A_1 (see Supporting Information). Typical concentration–time curves for the present consecutive reactions are shown in Figure S7 using the rate constants, which will be given later in Table 1. The first step of the consecutive reactions ends within 500 ns. Furthermore, the reaction curve of this first step is complicated because of the overlaps of the fast process. Accordingly, we determined the rate constant, λ_3 , from the kinetic analysis of the slower decay, which strictly followed first-order kinetics, by omitting the initial part of the reaction curve of the slow process. The pseudo-first-order rate constant, k_{obsd} , shown in Figure 6 corresponds to the rate constant, λ_3 .

In the present case, preequilibrium of the dead-end complex formation between $[\text{Cr}(\text{TMP})(\text{Cl})(\text{H}_2\text{O})]$ and an external ligand such as Py should be considered as in the case of the TPP complex.¹⁰ Furthermore, if another dead-end complex formation between $[\text{Cr}(\text{TMP})(\text{Cl})(\text{H}_2\text{O})]$ and an H_2O molecule (eq 11) is considered, the obtained pseudo-first-order rate constant is more satisfactorily explained.



The proposed structure of the dead-end complexes is shown in Chart 1. Taking the formation of these two dead-end complexes into account, the rate constants, k_{12} , k_{21} , and k_{23} , in the pseudo-first-order rate constant λ_3 are formulated as $k_{12} = k_{-\text{H}_2\text{O}}(1 + K_{\text{L}}[\text{L}] + K_{\text{H}_2\text{O}}[\text{H}_2\text{O}])^{-1}$, $k_{21} = k_{\text{H}_2\text{O}}[\text{H}_2\text{O}]$, and $k_{23} = k_{\text{L}}[\text{L}]$.

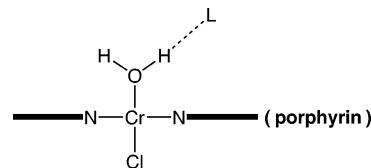
- (31) Matsen, F. A.; Franklin, J. L. *J. Am. Chem. Soc.* **1950**, *72*, 3337.
 (32) Moore, J. W.; Pearson, R. G. *Kinetics and Mechanism*; Wiley-Interscience Publications: New York, 1981.
 (33) The rate constant of the dissociation of the axial Py ligand from $[\text{Cr}(\text{TMP})(\text{Cl})(\text{Py})]$ was determined as 2.6 s^{-1} ($T = 25.0 \text{ }^\circ\text{C}$) in the kinetic study on the axial substitution reaction of $[\text{Cr}(\text{TMP})(\text{Cl})(\text{Py})]$ by 1-Melm in the toluene solution. These results will be published elsewhere.

Table 1. Kinetic and Thermodynamic Parameters^a for the Water Substitution Reaction of $[\text{Cr}(\text{porphyrin})(\text{Cl})(\text{H}_2\text{O})]$ by the Nitrogen Base L at $T = 25.0 \text{ }^\circ\text{C}^b$

	porphyrin	
	TMP	OEP
$k_{-\text{H}_2\text{O}}/\text{s}^{-1}$	6.96×10^6	4.86×10^5
$\Delta H_{-\text{H}_2\text{O}}^\ddagger$	43.9 ± 2.0	60.5 ± 1.3
$\Delta S_{-\text{H}_2\text{O}}^\ddagger$	33.3 ± 6.5	66.8 ± 4.5
$k_{\text{H}_2\text{O}}/\text{mol}^{-1} \text{ kg s}^{-1}$	1.39×10^9	1.52×10^9
$\Delta H_{\text{H}_2\text{O}}^\ddagger$	3.1 ± 1.3	6.6 ± 1.2
$\Delta S_{\text{H}_2\text{O}}^\ddagger$	-59.3 ± 4.2	-47.0 ± 3.9
$k_{\text{L}}/\text{mol}^{-1} \text{ kg s}^{-1}$	4.62×10^8 (L = Py)	7.42×10^8 (L = Py)
	3.88×10^8 (L = 3-CNPy)	5.56×10^8 (L = 1-Melm)
$\Delta H_{\text{L}}^\ddagger$	6.6 ± 1.5 (L = Py)	9.3 ± 1.3 (L = Py)
	8.0 ± 1.7 (L = 3-CNPy)	8.6 ± 1.3 (L = 1-Melm)
$\Delta S_{\text{L}}^\ddagger$	-56.8 ± 5.1 (L = Py)	-43.8 ± 4.4 (L = Py)
	-53.5 ± 5.6 (L = 3-CNPy)	-48.7 ± 4.2 (L = 1-Melm)
$K_{\text{L}}/\text{mol}^{-1} \text{ kg}$	8.30×10^2 (L = Py)	1.65×10^2 (L = Py)
	7.85×10 (L = 3-CNPy)	5.15×10^2 (L = 1-Melm)
$\Delta H_{\text{L}}^\circ$	-38.3 ± 2.0 (L = Py)	-29.9 ± 1.3 (L = Py)
	-29.6 ± 2.2 (L = 3-CNPy)	-28.7 ± 1.2 (L = 1-Melm)
$\Delta S_{\text{L}}^\circ$	-72.5 ± 6.5 (L = Py)	-57.8 ± 4.4 (L = Py)
	-62.9 ± 7.3 (L = 3-CNPy)	-44.2 ± 3.8 (L = 1-Melm)
$K_{\text{H}_2\text{O}}/\text{mol}^{-1} \text{ kg}$	4.92×10	<i>c</i>
$\Delta H_{\text{H}_2\text{O}}^\circ$	-32.8 ± 3.4	<i>c</i>
$\Delta S_{\text{H}_2\text{O}}^\circ$	-78 ± 11	<i>c</i>

^a $\Delta H/\text{kJ mol}^{-1}$; $\Delta S/\text{J mol}^{-1} \text{ K}^{-1}$. ^b Values of the rate and equilibrium constants were calculated by using the determined ΔH^\ddagger , ΔS^\ddagger , ΔH° , and ΔS° . ^c Term $K_{\text{H}_2\text{O}}$ is not necessarily included in the rate law to explain the kinetic results.

Chart 1



The $k_{\text{H}_2\text{O}}$ and $k_{-\text{H}_2\text{O}}$ terms included in eq 1 are identical with those in the present substitution reaction. The second term of the right-hand side of eq 2 should be modified because of the formation of the dead-end complex, $[\text{Cr}(\text{TMP})(\text{Cl})(\text{HOH}\cdots\text{OH}_2)]$, and the pseudo-first-order rate constant k_{obsd} in eq 2 can be rewritten as

$$k_{\text{obsd}} = k_{\text{H}_2\text{O}}[\text{H}_2\text{O}] + k_{-\text{H}_2\text{O}}(1 + K_{\text{H}_2\text{O}}[\text{H}_2\text{O}])^{-1} \quad (12)$$

The kinetic results of the slow process of the photoreaction of $[\text{Cr}(\text{TMP})(\text{Cl})(\text{Py})]$ as well as $[\text{Cr}(\text{TMP})(\text{Cl})(3\text{-CNPy})]$ (Figure S8) were simultaneously analyzed together with those of the photoreaction of $[\text{Cr}(\text{TMP})(\text{Cl})(\text{H}_2\text{O})]$ using a weighted-least-squares fitting calculation based on eqs 10 and 12. The kinetic and thermodynamic parameters obtained are listed in Table 1. Solid lines in Figures 2, 6, S6, and S8 were calculated using the kinetic parameters obtained. A similar calculation was applied to the slow process of $[\text{Cr}(\text{OEP})(\text{Cl})(\text{Py})]$ and $[\text{Cr}(\text{OEP})(\text{Cl})(1\text{-Melm})]$ and the photoreaction of $[\text{Cr}(\text{OEP})(\text{Cl})(\text{H}_2\text{O})]$, and the kinetic parameters obtained are shown in Table 1. The ligand concentration dependence of the obtained rate constant k_{obsd} for the OEP complexes is shown in Figures 2, S9, and S10.

The presence of the dead-end complex, $[\text{Cr}(\text{TMP})(\text{Cl})(\text{HOH}\cdots\text{OH}_2)]$, changes the formulation of k_{obsd} from eq 2 to eq 12. The contribution of the second term of the right-hand side of eq 12 to the rate constant k_{obsd} is shown by the

dotted lines in Figure 2. The dead-end complex formation clearly affects the kinetics for the recombination reaction between $[\text{Cr}(\text{TMP})(\text{Cl})]$ and H_2O . On the other hand, the formation of this type of dead-end complex is negligible for the OEP complex under the present experimental conditions probably due to a much smaller $K_{\text{H}_2\text{O}}$ value (see Table 1).

Quantum Yield Measurements. The quantum yield, Φ_{diss} , for the photodissociation of the axial ligand L (L = H_2O , Py, and 1-MeIm) from the OEP complex $[\text{Cr}(\text{OEP})(\text{Cl})(\text{L})]$ in toluene was determined by laser flash photolysis. The yield, Φ_{diss} , of $[\text{Cr}(\text{OEP})(\text{Cl})(1\text{-MeIm})]$ was evaluated from the yield, $\Phi_{\text{H}_2\text{O}}$, for the formation of the intermediate species, $[\text{Cr}(\text{OEP})(\text{Cl})(\text{H}_2\text{O})]$. Equation 13 represents the relationship between Φ_{diss} and $\Phi_{\text{H}_2\text{O}}$:

$$\Phi_{\text{diss}} = \Phi_{\text{H}_2\text{O}}(k_{\text{H}_2\text{O}}[\text{H}_2\text{O}] + k_{\text{L}}[\text{L}])k_{\text{H}_2\text{O}}^{-1}[\text{H}_2\text{O}]^{-1} \quad (13)$$

The initial transients observed at 29 ns after the laser pulse are the triplet states of $[\text{Cr}(\text{OEP})(\text{Cl})(1\text{-MeIm})]$ and $[\text{Cr}(\text{OEP})(\text{Cl})]$. After the completion of the fast process, the residual intermediate is solely ascribed to $[\text{Cr}(\text{OEP})(\text{Cl})(\text{H}_2\text{O})]$. Thus, the absorbance change ΔA obtained immediately after the disappearance of the initial transients is given by

$$\Delta A = \Phi_{\text{H}_2\text{O}}(\Delta\epsilon_1)I_{\text{abs}}N_{\text{A}}^{-1} \quad (14)$$

where I_{abs} , $\Delta\epsilon_1$, and N_{A} represent the number of photons absorbed by $[\text{Cr}(\text{OEP})(\text{Cl})(1\text{-MeIm})]$, the difference in the molar absorption coefficients between $[\text{Cr}(\text{OEP})(\text{Cl})(\text{H}_2\text{O})]$ and $[\text{Cr}(\text{OEP})(\text{Cl})(1\text{-MeIm})]$, and Avogadro's number, respectively. The value of $\Delta\epsilon_1$ was determined as $-1.14 \times 10^5 \text{ M}^{-1} \text{ cm}^{-1}$ at 444 nm from the absorption spectra of $[\text{Cr}(\text{OEP})(\text{Cl})(\text{L})]$ (L = H_2O and 1-MeIm) in toluene. A benzene solution of zinc(II) tetraphenylporphyrin, $[\text{Zn}(\text{TPP})]$, which has the same absorbance at the laser excitation wavelength (532 nm) as that of the toluene solution of $[\text{Cr}(\text{OEP})(\text{Cl})(1\text{-MeIm})]$, was used as a reference for the quantum yield measurements. When the benzene solution of $[\text{Zn}(\text{TPP})]$ is subjected to the laser pulse, the triplet excited state of $[\text{Zn}(\text{TPP})]$, which has the absorption band around the 470 nm region, is produced. The absorbance change, $\Delta A_{\text{T}(470\text{nm})}$, at 470 nm after the laser pulse is expressed as

$$\Delta A_{\text{T}(470\text{nm})} = \Phi_{\text{T}}\epsilon_{\text{T}}I_{\text{abs}}N_{\text{A}}^{-1} \quad (15)$$

where Φ_{T} (0.83) and ϵ_{T} ($7.3 \times 10^4 \text{ M}^{-1} \text{ cm}^{-1}$) are the triplet yield of $[\text{Zn}(\text{TPP})]$ and the molar absorption coefficient of the triplet excited state of $[\text{Zn}(\text{TPP})]$ at 470 nm, respectively.³⁴ From eqs 14 and 15, eq 16 is derived:

$$\Phi_{\text{H}_2\text{O}} = \Delta A(\Delta A_{\text{T}(470\text{nm})})^{-1}\epsilon_{\text{T}}(\Delta\epsilon_1^{-1})\Phi_{\text{T}} \quad (16)$$

The laser photolysis of $[\text{Cr}(\text{OEP})(\text{Cl})(\text{H}_2\text{O})]$ and $[\text{Cr}(\text{OEP})(\text{Cl})(\text{Py})]$ gives solely the initial transient species, $[\text{Cr}(\text{OEP})(\text{Cl})]$, immediately after the pulse. The formation of the triplet excited states could not be detected. Thus, the quantum yield

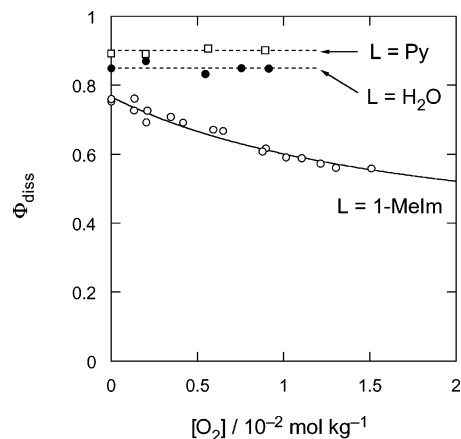


Figure 7. Effect of dioxygen on the quantum yield for the photodissociation of L from $[\text{Cr}(\text{OEP})(\text{Cl})(\text{L})]$ in toluene at 25.0 °C.

Φ_{diss} for the photodissociation of L from $[\text{Cr}(\text{OEP})(\text{Cl})(\text{L})]$ (L = H_2O and Py) is expressed as

$$\Phi_{\text{diss}} = \Delta A_{\text{diss}}(\Delta\epsilon_2^{-1})I_{\text{abs}}^{-1}N_{\text{A}} \quad (17)$$

where ΔA_{diss} and $\Delta\epsilon_2$ are the absorbance change just after laser excitation and the difference in the molar absorption coefficient between $[\text{Cr}(\text{OEP})(\text{Cl})]$ and $[\text{Cr}(\text{OEP})(\text{Cl})(\text{L})]$ (L = H_2O and Py) at a monitoring wavelength, respectively. The molar absorption coefficients of the five-coordinate intermediate $[\text{Cr}(\text{OEP})(\text{Cl})]$ at 470 nm was determined by the method previously described.⁶ Figure S11 shows the absorption spectrum of $[\text{Cr}(\text{OEP})(\text{Cl})]$ as well as those of $[\text{Cr}(\text{OEP})(\text{Cl})(\text{L})]$ (L = H_2O and Py). By using the benzene solution of $[\text{Zn}(\text{TPP})]$ as a reference, the quantum yield, Φ_{diss} , is readily obtained:

$$\Phi_{\text{diss}} = \Delta A_{\text{diss}}(\Delta A_{\text{T}(470\text{nm})})^{-1}\epsilon_{\text{T}}(\Delta\epsilon_2^{-1})\Phi_{\text{T}} \quad (18)$$

Figure 7 shows the dependence of Φ_{diss} on the concentration of dioxygen in the toluene solution. Dioxygen has no effect on the quantum yield of the photodissociation of H_2O and Py, while Φ_{diss} gradually decreases with an increase in the dioxygen concentration in the case of the 1-MeIm complex. The effect of dioxygen is also observed for the decay of the triplet excited state of $[\text{Cr}(\text{OEP})(\text{Cl})(1\text{-MeIm})]$ in toluene. The decay process was monitored at 480 nm where only the triplet excited state has an absorption band. Figure 8 shows the rate constant, k_{obsd} , for the decay of the triplet excited state as a function of the dioxygen concentration. The plot of k_{obsd} vs $[\text{O}_2]$ gives a straight line with an intercept:

$$k_{\text{obsd}} = k_{\text{T}} + k_{\text{q}}[\text{O}_2] \quad (19)$$

Here k_{T} and k_{q} are the rate constants for the decay of the triplet excited state in the absence of dioxygen and the bimolecular quenching rate constant of the excited state by dioxygen, respectively: $k_{\text{T}} = (2.4 \pm 0.1) \times 10^7 \text{ s}^{-1}$ and $k_{\text{q}} = (1.3 \pm 0.2) \times 10^9 \text{ mol}^{-1} \text{ kg s}^{-1}$ (25.0 °C).

As shown in Figure 7, Φ_{diss} observed for $[\text{Cr}(\text{OEP})(\text{Cl})(1\text{-MeIm})]$ asymptotically decreases with an increase in $[\text{O}_2]$ toward a constant value. This result suggests that the

(34) Hurley, J. K.; Sinai, N.; Linschitz, H. *Photochem. Photobiol.* **1983**, *38*, 9.

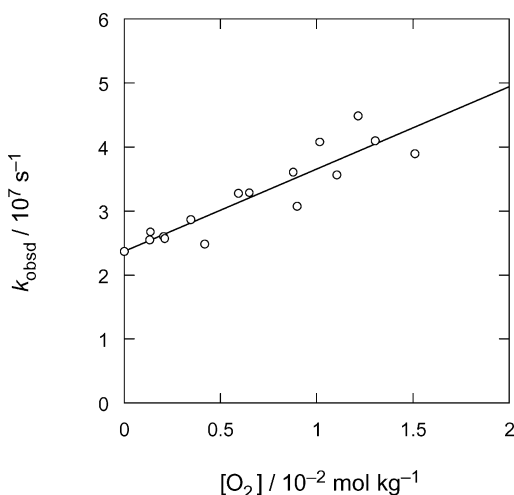


Figure 8. Plot of the first-order rate constant k_{obsd} for the decay of the 6T_1 state of $[\text{Cr}(\text{OEP})(\text{Cl})(1\text{-MeIm})]$ represented as a function of $[\text{O}_2]$ in toluene at 25.0 °C.

photodissociation of the ligand may occur in both the singlet and triplet excited states, the former with a very short lifetime ($\ll 1$ ns) and the latter with a lifetime long enough to be quenched by dioxygen. By assuming these mechanisms, Φ_{diss} can be expressed as

$$\begin{aligned}\Phi_{\text{diss}} &= \Phi_{\text{diss}}({}^4S_1) + \Phi_{\text{diss}}({}^6T_1) \\ &= \Phi_{\text{diss}}({}^4S_1) + \Phi({}^6T_1)k_{\text{diss}}(k_T + k_q[\text{O}_2])^{-1}\end{aligned}\quad (20)$$

where $\Phi_{\text{diss}}({}^4S_1)$, $\Phi_{\text{diss}}({}^6T_1)$, and $\Phi({}^6T_1)$ represent the quantum yields for the ligand dissociation at the 4S_1 and 6T_1 states and the formation of the triplet excited state, respectively. The solid line in Figure 7 is calculated using a least-squares fitting analysis with values of k_T and k_q obtained from Figure 8. The determined values are $\Phi_{\text{diss}}({}^4S_1) = (0.30 \pm 0.02)$ and $\Phi({}^6T_1)k_{\text{diss}}k_q^{-1} = (8.7 \pm 0.4) \times 10^{-3} \text{ mol kg}^{-1}$. Since Φ_{diss} determined in the absence of oxygen is 0.77, the quantum yield of the ligand dissociation reaction in the triplet excited state, $\Phi_{\text{diss}}({}^6T_1)$, can be estimated to be 0.47 from eq 20.

Discussion

Electronic State of the Complex and Reactivity of the Photodissociation of the Axial Ligand. One of the most outstanding characteristics of the photochemistry of the Cr(III) porphyrin complexes is the efficiency of the photodissociation of the axial ligand. The reactive excited states of metalloporphyrins with the first-row transition metals are expected to be (1) intraligand S_1 state, (π, π^*) , (2) intraligand T_1 state, (π, π^*) , (3) ligand field excited states, (d, d) , (4) ligand to metal charge-transfer states, (π, d) , and (5) metal to ligand charge transfer states, (d, π^*) .¹ In particular, as mentioned for the porphyrin complexes of transition metals such as Fe(II), Co(II), Co(III), and Ni(II),^{35–44} the low-lying

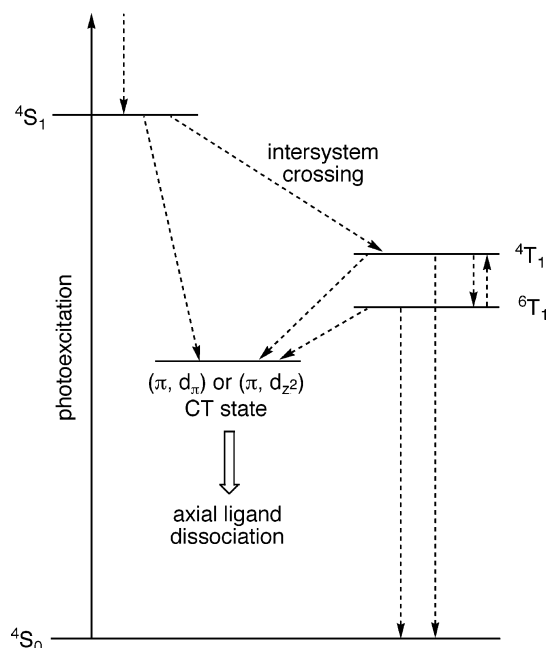


Figure 9. Energy level diagram for the Cr(III) porphyrin complexes in toluene.

(π, d_z^2) charge transfer and (d, d_z^2) excited states may be responsible for the dissociation of σ -bonded axial ligands because increasing electron density in the d_z^2 orbital will weaken the bond between the metal and axial ligand. In the case of the chromium(III) porphyrins, theoretical investigations revealed that vacant d_z^2 and half-filled d_{xy} , d_{yz} , and d_{xz} orbitals of a chromium atom are located between the HOMO $a_{2u}(\pi)$ and LUMO $e_g(\pi^*)$ orbitals of the porphyrin ring in energy, whereas an empty $d_{x^2-y^2}$ orbital lies well above the $e_g(\pi^*)$ orbital.² Recent transient absorption and resonance Raman studies suggest that the normally emissive excited triplet (π, π^*) of the chromium(III) porphyrins has a radiationless transition pathway via the low-lying (π, d_T) CT state.¹¹ In this study, the quenching experiment using dioxygen revealed that both 4S_1 and 6T_1 excited states are responsible for the photodissociation of the axial ligand. Presumably, the dissociation of the axial ligand occurs from the (π, d_T) or (π, d_z^2) CT states, which locate lower in energy than the 4S_1 and 6T_1 excited states. Figure 9 shows the electronic energy dissipation diagram of the Cr(III) porphyrin complexes. By assuming that the dissociation of the axial ligand at the CT states occurs with an efficiency of unity, k_{diss} in eq 20 is interpreted as the rate constant from the triplet excited state to the CT state.

Quantum yield for the photodissociation of the axial ligand is influenced by the nature of the porphyrin and axial ligands

(35) Lavalette, D.; Tetreau, C.; Momenteau, M. *J. Am. Chem. Soc.* **1979**, *101*, 5395.

(36) Dixon, D. W.; Kirmaier, C.; Holten, D. *J. Am. Chem. Soc.* **1985**, *107*, 808.

(37) Maillard, P.; Schaeffer, C.; Tetreau, C.; Lavalette, D.; Lhoste, J.-M.; Momenteau, M. *J. Chem. Soc., Perkin Trans. 2* **1989**, 1437.

(38) Tetreau, C.; Lavalette, D.; Momenteau, M. *J. Am. Chem. Soc.* **1983**, *105*, 1506.

(39) Tait, C. D.; Holten, D.; Gouterman, M. *Chem. Phys. Lett.* **1983**, *100*, 268.

(40) Tait, C. D.; Holten, D.; Gouterman, M. *J. Am. Chem. Soc.* **1984**, *106*, 6653.

(41) Hoshino, M.; Kogure, M.; Asano, K.; Hinohara, T. *J. Phys. Chem.* **1989**, *93*, 6655.

(42) Kim, D.; Holten, D. *Chem. Phys. Lett.* **1983**, *98*, 584.

(43) Kim, D.; Kirmaier, C.; Holten, D. *Chem. Phys.* **1983**, *75*, 305.

(44) Rodriguez, J.; Holten, D. *J. Chem. Phys.* **1990**, *92*, 5944.

coordinated to the central metal. In a previous study, we found that [Cr(TPP)(Cl)(1-MeIm)] does not dissociate the axial 1-MeIm by the laser flash photolysis.⁹ However, the OEP complex, [Cr(OEP)(Cl)(1-MeIm)], releases 1-MeIm with the quantum yields of 0.30 ($\Phi_{\text{diss}}(^4\text{S}_1)$) and 0.47 ($\Phi_{\text{diss}}(^6\text{T}_1)$). Such a difference in the quantum yield for the photodissociation of the axial ligand was also seen for the Py complexes, [Cr(TPP)(Cl)(Py)] and [Cr(OEP)(Cl)(Py)].⁴⁵ These findings indicate that the conversion of the porphyrin-centered $^4\text{S}_1$ excited state to the states having dissociative character competes with the rate of the intersystem crossing from $^4\text{S}_1$ to $^4\text{T}_1$, and the former process should be more efficient for the OEP complex as compared with the TPP complex. There should be substantial differences in the porphyrin molecular orbital between OEP and TPP that affect the electron density on the metal and the kinetics of the decay of the excited states of the complexes.

The rate constant of the axial ligand dissociation at the triplet excited states can be estimated from the quantum yield measurements. The quantum yield, $\Phi_{\text{diss}}(^6\text{T}_1)$, of [Cr(OEP)(Cl)(1-MeIm)] is markedly larger than that of [Cr(TPP)(Cl)(1-MeIm)]: $\Phi_{\text{diss}}(^6\text{T}_1) = 0.47$ for [Cr(OEP)(Cl)(1-MeIm)] and $\Phi_{\text{diss}}(^6\text{T}_1) < 0.01$ for [Cr(TPP)(Cl)(1-MeIm)].⁹ From eq 20, the quantum yield, $\Phi_{\text{diss}}(^6\text{T}_1)$, in the absence of dioxygen is written as

$$\Phi_{\text{diss}}(^6\text{T}_1) = [\Phi(^6\text{T}_1)]k_{\text{diss}}k_{\text{T}}^{-1} \quad (21)$$

The term k_{T} can be expressed as $k_{\text{T}} = k_{\text{diss}} + k$, where k is the rate constant for the decay from the triplet excited state to the ground state in the dioxygen-free toluene solution. For [Cr(TPP)(Cl)(1-MeIm)], we obtain $k_{\text{diss}} < 9 \times 10^4 \text{ s}^{-1}$ (25.0 °C) using the values of $\Phi(^6\text{T}_1) = 0.88$, $\Phi_{\text{diss}}(^6\text{T}_1) < 0.01$, and $k_{\text{T}} = 7.75 \times 10^6 \text{ s}^{-1}$ at 25.0 °C.⁹ In the case of the OEP complex, the k_{diss} value can be estimated from the decay rate constant of the $^6\text{T}_1$ excited state in the dioxygen-free toluene solution ($k_{\text{diss}} + k = 2.4 \times 10^7 \text{ s}^{-1}$ at 25.0 °C) and that in the polystyrene film ($k = 3.7 \times 10^6 \text{ s}^{-1}$ at 25.0 °C) on the assumption that the rate constant k is almost the same for both conditions, giving the k_{diss} value of $2.0 \times 10^7 \text{ s}^{-1}$ at 25.0 °C.⁴⁶ The rate constant, k_{diss} , for the dissociation of the axial 1-MeIm via the triplet excited state of the OEP complex is at least 200 times larger than that of the TPP complex. In contrast, we could not find appreciable difference in the rate constant for the axial 1-MeIm dissociation reaction at the ground state between [Cr(TPP)(Cl)(1-MeIm)] and [Cr(OEP)(Cl)(1-MeIm)]. The former gives the rate constant $2.6 \times 10^{-2} \text{ s}^{-1}$ (25.0 °C),²³ and the latter, $7.4 \times 10^{-2} \text{ s}^{-1}$ (25.0 °C).⁴⁷ It

is concluded that the difference in the porphyrin structure affects the reactivity of the axial ligand dissociation in the excited state more markedly than in the ground state.

Another aspect that should be pointed out is the difference in the photodissociation efficiency between the Py and 1-MeIm complexes. The quantum yield of the photodissociation of Py is larger than that of 1-MeIm for both cases of TPP and OEP. These differences are considered to originate from the nature of the bond between the metal and axial ligand. The molecular structure of the complex clearly demonstrates that the bond length between the chromium and the axial Py nitrogen atoms in [Cr(TPP)(Cl)(Py)] ($r_{\text{Cr-N(Py)}} = 2.140(5) \text{ \AA}$) is longer than the corresponding bond length of 2.103(4) Å in [Cr(TPP)(Cl)(1-MeIm)].^{6,24} This result can reasonably be explained by the steric effect: the six-membered pyridine ring at the axial site of the metalloporphyrins is expected to suffer greater steric hindrance than the five-membered imidazole ring due to greater repulsion between the pyridine α -hydrogen atoms and the porphyrin core. Judging from the bond lengths, we consider that the bond dissociation energy of the axial ligand of [Cr(porphyrin)(Cl)(Py)] should be smaller than that of [Cr(porphyrin)(Cl)(1-MeIm)], and thus, the quantum yield for the photodissociation of the former is much larger than that of the latter.

Steric Effect on the Axial Substitution Reaction. As shown in Table 1, the five-coordinate intermediate, [Cr(porphyrin)(Cl)], produced by the photodissociation of the axial ligand has a high reactivity toward the ligand association reaction. The small activation enthalpy and negative activation entropy for the axial ligand binding of Cr(III) porphyrins indicate that the energy required for orientation of the reacting molecules in a favorable configuration seems small, like other metalloporphyrins with very large rate constants (in the range of 10^8 – $10^9 \text{ mol}^{-1} \text{ kg s}^{-1}$) for the axial ligand rebinding for Fe(II)^{35–37} and Co(III)^{39–41} porphyrins. Due to the high reactivity of the five-coordinate intermediate, there exists little difference in the kinetic parameters of the ligand rebinding reaction between OEP and TMP complexes.

It was found that the peripheral substituents on the porphyrin ligand affect the dynamics of the axial water dissociation reaction from [Cr(porphyrin)(Cl)(H₂O)]. The $k_{-\text{H}_2\text{O}}$ value for the TMP complex is greater than that of the OEP complex by a factor of 20. The substituent effect can also be found in the activation enthalpy; i.e., $\Delta H^\ddagger_{-\text{H}_2\text{O}}$ is 43.9 kJ mol⁻¹ for the TMP complex and 60.5 kJ mol⁻¹ for the OEP complex. A similar effect was found for the water-exchange reaction of water-soluble iron(III) porphyrins in aqueous solution studied by a high-pressure ¹⁷O NMR technique.⁴⁸ The α -methyl groups of the *meso*-aryl groups of the porphyrin in [Fe(TMPS)(H₂O)₂]³⁻ (TMPS = 5,10-,15,20-tetrakis(sulfonatomesityl)porphyrin) enhance the rate of the axial water exchange reaction by a factor of 10 in comparison with [Fe(TPPS)(H₂O)₂]³⁻ (TPPS = 5,10,15,20-tetrakis(4-sulfonatophenyl)porphyrin). A larger activation

(45) Quantum yields of the Py dissociation, $\Phi_{\text{diss}}(^4\text{S}_1)$ and $\Phi_{\text{diss}}(^6\text{T}_1)$, were determined to be 0.18 and 0.47 for [Cr(TPP)(Cl)(Py)],⁹ while Py dissociates almost quantitatively at the excited state derived from $^4\text{S}_1$ for [Cr(OEP)(Cl)(Py)] ($\Phi_{\text{diss}}(^4\text{S}_1) = 0.89$).

(46) In this study, we could not determine the triplet yield, $\Phi(^6\text{T}_1)$, of [Cr(OEP)(Cl)(1-MeIm)] from the transient spectrum observed immediately after the pulse, and therefore, the k_{diss} value cannot be calculated directly. We, however, can estimate the triplet yield from the assumption of $\Phi_{\text{diss}}(^4\text{S}_1) + \Phi(^6\text{T}_1) \sim 1.0$. From $\Phi_{\text{diss}}(^4\text{S}_1) = 0.3$, $\Phi(^6\text{T}_1)$ is obtained as ca. 0.7. With the use of eq 21, $\Phi(^6\text{T}_1) = 0.7$, $\Phi_{\text{diss}}(^6\text{T}_1) = 0.47$, and $k_{\text{T}} = 2.4 \times 10^7 \text{ s}^{-1}$, k_{diss} is calculated as $1.6 \times 10^7 \text{ s}^{-1}$ at 25 °C, which is in good agreement with the value of $k_{\text{diss}} = 2.0 \times 10^7 \text{ s}^{-1}$ mentioned in the text.

(47) Unpublished data.

(48) Schnepfensieper, T.; Zahl, A.; van Eldik, R. *Angew. Chem., Int. Ed.* **2001**, *40*, 1678.

volume as well as a smaller activation enthalpy due to the bulky α -methyl groups has been discussed in terms of the effect of steric decompression on a dissociative activation processes.

On the other hand, the acceleration effect due to the bulky α -methyl groups on the peripheral phenyl groups was not observed for the dissociation reaction of the axial ligand L from [Cr(porphyrin)(Cl)(L)] (porphyrin = TPP, OEP, TMP; L = Py, 1-MeIm); i.e., the dissociation rate constants of Py and 1-MeIm at 25.0 °C were determined to be 8.2 and $2.6 \times 10^{-2} \text{ s}^{-1}$ for the TPP complex,²³ 19 and $7.4 \times 10^{-2} \text{ s}^{-1}$ for the OEP complex,⁴⁵ and 2.6 and $2.4 \times 10^{-2} \text{ s}^{-1}$ for the TMP complex,⁴⁷ respectively. These findings indicate that the acceleration effect on the H₂O dissociation reaction of the TMP complex may be caused by the difference in the environment of the axial H₂O ligand; i.e., the more hydrophobic environment of the axial coordinating site of the TMP complex due to the α -methyl groups makes the H₂O ligand less stable, and this effect causes the faster rate of the water dissociation reaction.

Conclusions

Photochemical reactions of [Cr(OEP)(Cl)(L)] and [Cr(TMP)(Cl)(L)] (L = H₂O, Py, 1-MeIm) were investigated in the toluene solution using a nanosecond laser flash photolysis technique. The laser photolysis of [Cr(porphyrin)(Cl)(L)] in toluene generates the triplet excited state of the six-coordinate complex as well as a coordinately unsaturated complex, [Cr(porphyrin)(Cl)]. On the basis of the effect of dioxygen on the quantum yield, the photodissociation of the axial ligand was confirmed to occur at the dissociative states via both the excited ⁴S₁ and ⁶T₁ (and/or ⁴T₁) states. For the Py and 1-MeIm complexes, the transient spectra observed immediately after the laser pulse exhibit the biphasic decay. The fast process is attributed to the deactivation of the ⁶T₁

and ⁴T₁ states and the binding of the axial ligand L or water molecules to the five-coordinate [Cr(porphyrin)(Cl)]. The slow decay process is due to the axial H₂O ligand substitution reaction of the transient species, [Cr(porphyrin)(Cl)(H₂O)], by the ligand L to regenerate the initial complex. The mechanism of the axial H₂O substitution reaction was confirmed to be the dissociative mechanism. The laser photolysis of [Cr(porphyrin)(Cl)(H₂O)] in toluene causes the dissociation of the axial H₂O to yield [Cr(porphyrin)(Cl)], followed by the recombination of the H₂O molecule, and any other excited states were not observed. The reactivity of the excited states of the Cr(III) porphyrin markedly depends on the nature of the porphyrin ligand. Actually, the triplet excited state of [Cr(OEP)(Cl)(1-MeIm)] is found to dissociate the axial ligand L more efficiently than that of [Cr(TPP)(Cl)(1-MeIm)]. This finding is explained by assuming that the OEP complex undergoes the conversion from the triplet states to the dissociative excited states much faster than the TPP complex. The dissociative excited states responsible for the ligand dissociation are suggested to be the CT excited states.

Supporting Information Available: Figures reporting the UV–visible absorption spectra of [Cr(OEP)(Cl)(L)] (L = H₂O, 1-MeIm, Py) and [Cr(TMP)(Cl)(L)] (L = H₂O, Py), transient spectra of [Cr(OEP)(Cl)(L)] (L = H₂O, 1-MeIm), ligand concentration dependence of k_{obsd} for the reaction of [Cr(TMP)(Cl)(H₂O)] with Py in toluene, concentration–time curves for the consecutive reactions, ligand concentration dependence of k_{obsd} for the reaction of [Cr(TMP)(Cl)(H₂O)] with 3-CNPY in toluene, ligand concentration dependence of k_{obsd} for the reaction of [Cr(OEP)(Cl)(H₂O)] with L (L = Py, 1-MeIm) in toluene, and the UV–visible absorption spectrum of the five-coordinate [Cr(OEP)(Cl)] and rate equations for the consecutive reactions. This material is available free of charge via the Internet at <http://pubs.acs.org>.

IC0342696